Journal of Hydroscience and Hydraulic Engineering
Vol. 21, No.2 November, 2003, 37-45

UNSATURATED WATER FLOW AND SOLUTE TRANSPORT IN ARTIFICIALLY DISTRIBUTED HYDRAULIC CONDUCTIVITY FIELD

By

Kei NAKAGAWA

Kagoshima University, 1-21-24 Korimoto, Kagoshima 890-0065, Japan

Masahide IWATA

Technical Research Institute, Maeda Corporation, 1-39-16 Asahicho, Nerimaku, Tokyo 179-8914, Japan

Jiro CHIKUSHI

Kyushu University, 6-10-1 Hakozaki, Higashi-ku, Fukuoka 812-8581, Japan

and

Kazuro MOMII

Kagoshima University, 1-21-24 Korimoto, Kagoshima 890-0065, Japan

SYNOPSIS

Hydraulic parameters, such as hydraulic conductivity and dispersivity, are heterogeneously distributed in natural soils and aquifers. They greatly affect water and solute transport properties. For this reason it is important to characterize the scale of variation. In this study, laboratory experiments and numerical simulations were carried out to understand simultaneous solute transport and soil water flow in an unsaturated artificially distributed hydraulic conductivity field. The time domain reflectometry (TDR) method was used to measure water content and electric conductivity in the experiments. The method of characteristics (MOC) was applied to the numerical simulations of solute transport. Preferential water flow and solute transport were observed both in numerical and experimental results due to the heterogeneous structure of the porous media. The numerical prediction of tracer movement partially agreed with experimental results. This provides evidence of the effectiveness of the numerical model presented here. Further laboratory and numerical studies are needed to predict preferential flow more precisely.

INTRODUCTION

Most contaminants that infiltrate from the soil surface reach the groundwater table through the unsaturated zone and cause groundwater pollution. Since hydraulic parameters such as hydraulic conductivity and dispersivity in soils are heterogeneously distributed, the contaminants move downwards through the soil in a complicated infiltration process along with water flow. This process results in preferential water flow and solute transport. Evaluation of preferential flow and transport due to the heterogeneous distribution of hydraulic parameters is useful when considering countermeasures against soil and groundwater pollution. Thus, many theoretical, numerical, and experimental studies have been carried out to investigate the effects of heterogeneity on the water flow and solute transport [1-3]. Sakamoto systematically investigated soil formation mechanisms, shape and fractal properties of the water channel flow [4, 5]. However, he examined only water channel flow caused by capillary fingering, not the preferential flow due to heterogeneity of hydraulic parameters. Nakagawa *et al.* dealt with the macroscopic dispersion of non-reactive solute for the heterogeneous field in terms of hydraulic conductivity for saturated conditions [6-8]. However, the effects of heterogeneity on the solute transport under unsaturated conditions were not discussed. Yeh and Harvey described the concept of effective hydraulic conductivity based on one-dimensional vertical column experiment [3]. Since the smallest hydraulic conductivity in the flow domain restricts the water flow in one-dimension, the effect of heterogeneity on the water flow was not examined in detail. Wildenschild and Jensen investigated experimentally and numerically the effective

hydraulic conductivity of a two-dimensional heterogeneous flow field [9, 10]. Despite these efforts, the effect of heterogeneity on solute transport has not been fully elucidated, especially for the unsaturated water flow regime.

The purpose of this study is to present experimental results of water and solute behavior in two-dimensional unsaturated heterogeneous porous media and to examine the accuracy of a numerical model. Time domain reflectometry (TDR) probes were used to measure simultaneously soil moisture and electric conductivity (EC) in laboratory experiments. For the numerical simulation, the method of characteristics (MOC) was applied to solve the solute transport equation [11].

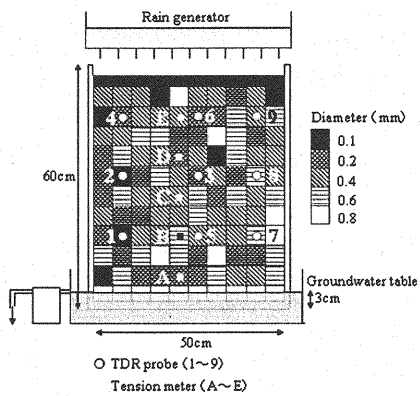

Figure 1 Experimental set-up

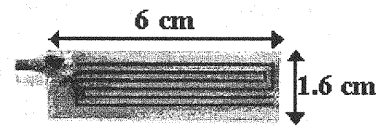

Figure 2 TDR probe

SOLUTE TRANSPORT EXPERIMENT IN AN UNSATURATED HETEROGENEOUS MEDIA

Experimental Method and Set-up

Figure 1 shows a schematic illustration of the experimental set-up. An experimental box (60×50×10 cm) of vinyl chloride was used. The bottom of the box was connected to an effluent box (12×62×22 cm) by a wire net. The effluent water was collected at 6 cm above the bottom of the effluent box. This position is as same as 3 cm above the bottom of the experimental box. The experimental box was filled with 5 sizes of glass beads to represent the heterogeneous porous medium. The heterogeneous medium was divided into 5×5 cm sized blocks with different homogeneous glass beads.

The arrangement of the blocks was determined by the following procedure: Firstly, we assumed a logarithmic distribution of saturated hydraulic conductivity according to

$$Y = \overline{Y} + \sigma_Y \cdot \varepsilon \qquad (1)$$

where Y is log-transformed hydraulic conductivity (Y=log k_S, where k_S is saturated hydraulic conductivity), σ_Y is standard deviation and $\overline{Y}$ is a mean value of Y. In this study, $\overline{Y}$=-1.05 and σ_Y=0.45 were used due to k_S distributions of the glass beads used in following experiment. To randomize k_S, 100 random numbers of normal distribution (mean 0, variance 1) were generated representing ε in equation (1). The obtained order of k_S values was arbitrarily redistributed into a two-dimensional arrangement of blocks. The hydraulic conductivity k_S of each block was categorized into 5 orders of magnitude. To homogenize the water flow at boundaries, a 3 cm thick layer of the smallest size beads (0.1 mm) was put at the top of the experimental box, and a 4 cm thick layer of the largest size beads (0.8 mm) was put at the bottom of the box. The water table was kept in the 0.8 mm beads layer.

TDR probes were installed according to observation points 1 to 9 in Figure 1, to measure soil moisture and electric conductivity (EC). The printed circuit board was set to be parallel to the flow direction. Tensiometers were also installed according to observation points A to E, to measure pressure head. Figure 2 shows the used TDR probe of printed circuit board (6×1.6×0.1 cm). In the board, actual transmission length of the electric magnetic wave is 15.5 cm. All probes were calibrated for each size of glass beads. The rainfall simulator made from vinyl chloride with porous plate and needles (0.5 mm) was put over the experimental box.

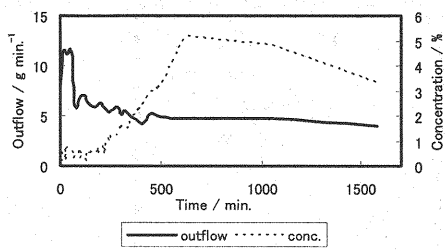

Figure 3 Experimental results of change in concentration and flux of effluent water

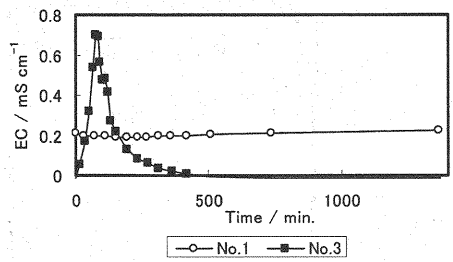

Figure 4 Experimental results of change in bulk electric conductivity

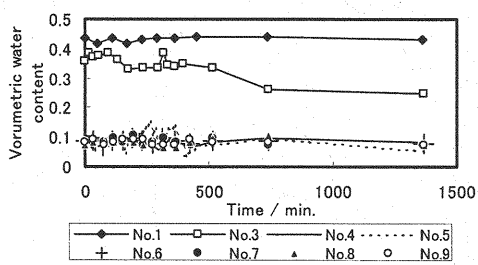

Figure 5 Experimental results of change in volumetric water content

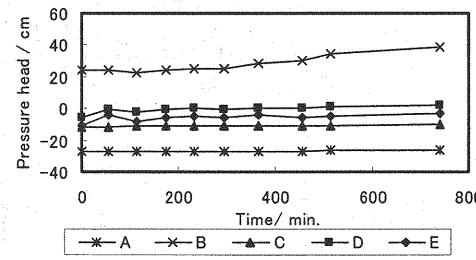

Figure 6 Experimental results of change in pressure head

The water and solute application procedure was as follows:

1) The effluent water box was initially filled with de-ionized water, and the water table was kept at a 3 cm level from the bottom of the box.
2) De-ionized water was applied to the surface of the medium through the artificial rainfall simulator, with 10 mm h^{-1}.
3) When the infiltrating water front reached the bottom of the experimental box, the rainfall simulator was removed and a 5 g L^{-1} NaCl solution was sprayed over the surface of the glass beads as a uniformly applied tracer. The total amount of tracer was 500 mL.
4) When the applied tracer had infiltrated, the artificial rain water application was resumed.
5) The experiment was finished when the NaCl concentration of the effluent water approached zero.

To visualize the movement of the tracer, a new coccin dye (Acid Red 18 from Kiriya Chemical Co. Ltd.) was used. The distribution of the tracer was photographed by means of a digital camera at fixed time intervals.

Experimental Results and Discussion

Figure 3 shows NaCl concentration and effluent water flux from the bottom of the experimental box. The concentration was obtained from the measured electric conductivity. A peak in the effluent water flux was observed during a 10 to 65 minutes range after the injection of tracer. This indicates that water originally contained in the box was pushed out by the injected tracer. After this peak, the flux was approximately constant. The concentration reached a peak value after about 500 min and then gradually decreased.

Figure 4 shows bulk electric conductivity with time in the porous medium. At observation point 3, the EC shows a pronounced peak in the 65 to 90 minutes range and then decreases gradually. At point 1, an almost constant EC was observed from the initial stage of the experiment. Since this constant value was the same as the EC of the effluent water, the concentration and water content at point 1 could have been affected by capillary rise from the water table. At other observation points, tracer values could not be detected. Furthermore, the dye showed that the tracer did not flow through these points.

Figure 5 shows the variation of volumetric water content with time. At point 1, the water content was constant from the initial stage of the experiment, and was probably in equilibrium with static capillary pressure from the water table. Relatively high water content was observed in the range of 0.3 to 0.4 $m^3 m^{-3}$ at point 3. This may have been caused by deviation of water from the area around observation point 3. At observation points 4 to 9, water contents were approximately constant.

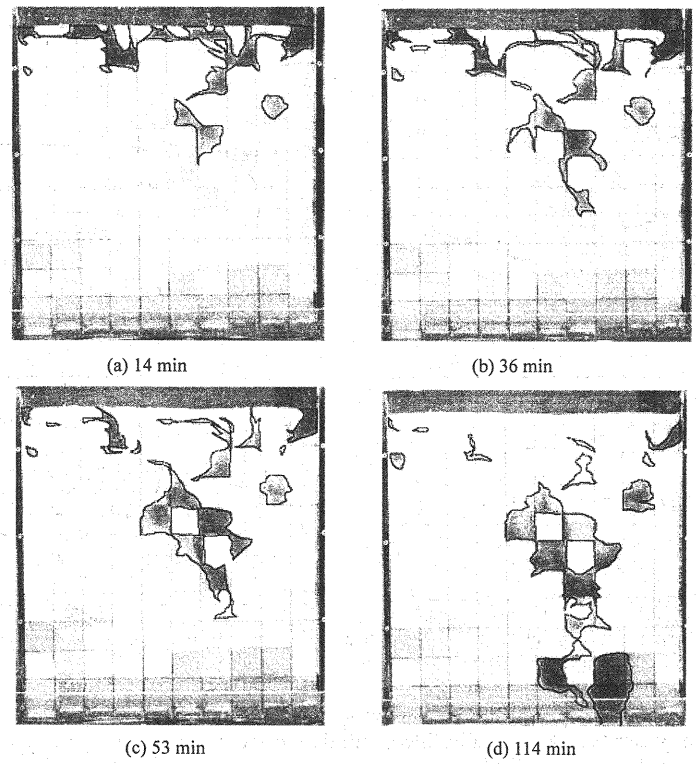

(a) 14 min (b) 36 min

(c) 53 min (d) 114 min

Figure 7 Infiltration process of dye (experiment)

Figure 6 shows pressure head variation at 5 observation points. Points A and C showed negative pressure, while point B showed positive pressure. Below point C, some points indicated almost saturation, while other points displayed unsaturated conditions. This suggests that infiltration from the surface generated preferential flow due to field heterogeneity. The same phenomenon was confirmed by observation of capillary rise from the water table. Preferential capillary rise was also found as a wetting front in heterogeneous profiles by making detailed observations.

Figure 7 shows the movement of the tracer during infiltration. The main part of the tracer at first moved preferentially to the right side of the visible experimental box side, and then moved downwards to the bottom of the experimental box. The preferential flow was caused by the low hydraulic conductivity volumes in the porous medium. For saturated conditions, it may be assumed that, in general, water will infiltrate mainly through macropores (large hydraulic conductivity zone), while for unsaturated conditions, water will preferentially flow through the finer matrix (low hydraulic conductivity zone) [12]. This phenomenon could account for the present experimental results.

ANALYSIS OF SOLUTE TRANSPORT IN THE UNSATURATED HETEROGENEOUS FIELD BY NUMERICAL SIMULATION

Numerical Model

The two-dimensional unsaturated water flow equation and the advection-dispersion equation were used for making the analysis. The groundwater flow equation is represented by

$$(c_W(\theta) + \beta S_s)\frac{\partial h}{\partial t} = -\frac{\partial u}{\partial x} - \frac{\partial v}{\partial y} \tag{2}$$

$$u = -k(\theta)\frac{\partial h}{\partial x} \tag{3}$$

$$v = -k(\theta)\left(\frac{\partial h}{\partial y} + 1\right) \tag{4}$$

where $k(\theta)$ is unsaturated hydraulic conductivity (L T^{-1}), t is time (T), h is pressure head (L), u and v are the Darcy velocity for the x and y directions (L T^{-1}), respectively, S_s is the specific storage coefficient (L^{-1}), θ is volumetric water content, $c_w(\theta)$ is the specific moisture capacity, and β is a dummy variable that takes the value 1 for the saturated zone and the value 0 for the unsaturated zone.

The solute transport equation is represented by

$$\begin{aligned} &\frac{\partial(\theta C)}{\partial t} + \frac{\partial(uC)}{\partial x} + \frac{\partial(vC)}{\partial y} = \\ &\frac{\partial}{\partial x}\left(D_{xx}\frac{\partial(\theta C)}{\partial x} + D_{xy}\frac{\partial(\theta C)}{\partial y}\right) \\ &+\frac{\partial}{\partial y}\left(D_{yx}\frac{\partial(\theta C)}{\partial x} + D_{yy}\frac{\partial(\theta C)}{\partial y}\right) \end{aligned} \tag{5}$$

where C is solute concentration. According to Huyakorn and Pinder [13], dispersion coefficients D_{xx}, D_{xy}, D_{yx}, and D_{yy} (L^2 T^{-1}) can be represented by the following equations as the sum of velocity dependent dispersion and molecular diffusion

$$D_{xx} = \frac{\alpha_L u'^2}{V} + \frac{\alpha_T v'^2}{V} + D_M \tag{6}$$

$$D_{yy} = \frac{\alpha_T u'^2}{V} + \frac{\alpha_L v'^2}{V} + D_M \tag{7}$$

$$D_{xy} = D_{yx} = \frac{(\alpha_L - \alpha_T)u'v'}{V} \tag{8}$$

where D_M is molecular diffusion coefficient of water (L^2 T^{-1}), $V = \sqrt{u'^2 + v'^2}$, u' and v' are pore water velocities of x and y directions (L T^{-1}), respectively, α_L is longitudinal dispersivity (L), and α_T is transversal dispersivity (L), which is assumed to be α_T=0.1α_L.

For the calculation of unsaturated flow, we need to know the relationship for volumetric water content vs. pressure head (characteristic moisture curve) and unsaturated hydraulic conductivity vs. specific moisture capacity. In this study, the characteristic moisture curve was determined by fitting the equation of van Genuchten [14] to the results of a soil column experiment.

$$\begin{aligned} &S_0 = \frac{\theta - \theta_r}{\theta_s - \theta_r}, \quad S_e = \left[\frac{1}{1 + (\alpha|h|)^n}\right]^m \\ &k_r = S_0^{1/2}\left\{1 - \left(1 - S_e^{1/m}\right)^m\right\}^2 \\ &C_w = \frac{\alpha \cdot m(\theta_s - \theta) S_e^{1/m}\left(1 - S_e^{1/m}\right)^m}{1 - m} \end{aligned} \tag{9}$$

where θ_r is residual water content, θ_s is saturated water content and α, m and n are the coefficients of van Genuchten formula. The characteristic moisture curve is shown in Figure 8. Table 1 shows the resulting unsaturated parameters, hydraulic conductivities, and longitudinal dispersivities.

Calculation Methods and Numerical Conditions

To solve the groundwater flow equation (2), an iterative calculation was carried out by the implicit finite difference method. To solve the solute transport equation (5), the method of characteristics (MOC) was applied. The simulation area was 50.00 cm in x-direction and 53.75 cm in y-direction with a grid interval of 1.25 cm.

Table 1 Unsaturated parameters of glass beads

Diameter/mm	k_s / cm s^{-1}	α_L / cm	θ_r	θ_s	α	n
0.1	8.92×10^{-3}	3.67×10^{-3}	0.000	0.412	0.022	19.0
0.2	2.98×10^{-2}	7.34×10^{-3}	0.000	0.394	0.029	7.51
0.4	8.57×10^{-2}	1.47×10^{-2}	0.029	0.394	0.074	10.7
0.6	2.16×10^{-1}	2.20×10^{-2}	0.028	0.407	0.107	8.16
0.8	3.58×10^{-1}	2.93×10^{-2}	0.027	0.380	0.156	7.75

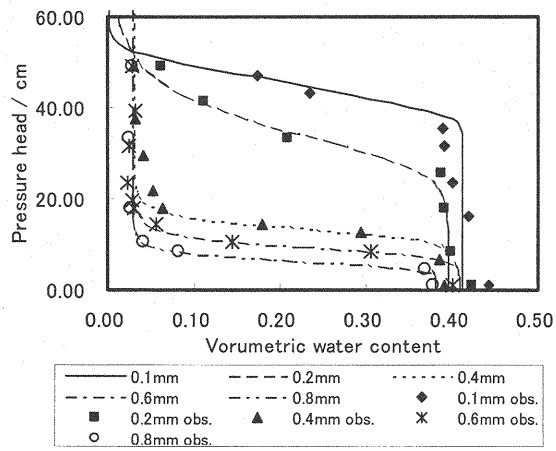

Figure 8 Characteristic moisture curves for glass beads

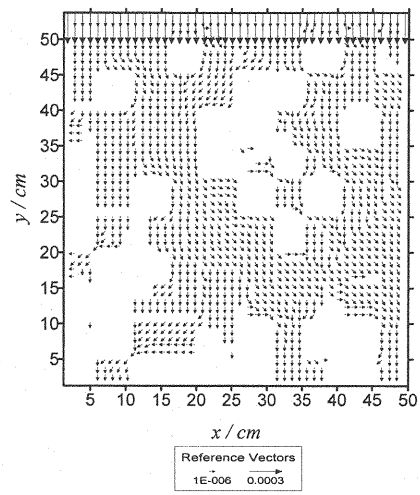

Figure 9 Numerical results of velocity vector distribution

For the initial conditions of pressure head, a hydrostatic pressure distribution was selected for the entire numerical domain. For the upper surface, a 100 % concentration was applied as initial condition. At all other grid points the initial condition for concentration was set at 0 %.

During water application, the upper surface boundary condition was set at a constant pressure head of 1.0 cm. During other periods, the artificial rain water flux (10 mm h^{-1}) boundary was applied. For the lower boundary condition, a constant pressure was applied and left and right boundaries were impermeable. During tracer application, the concentration boundary of the upper surface was set at a constant value of 100 % and during other periods, a 0 % condition was applied. Lower, left, and right boundary conditions had no gradient of concentration.

Numerical results and discussion

Figure 9 shows the calculated results of the velocity distribution before the tracer application. Water bypassed low hydraulic conductivity zones and tended to flow to high hydraulic conductivity zones.

Figure 10 shows the calculated concentration of tracer in the experimental box. The tracer also bypassed low hydraulic conductivity zones. The tracer moved along the flow paths of water. At the upper part of the low hydraulic conductivity zone, the tracer stagnated for a while and a high concentration was observed. This tendency agrees in a qualitative way with experimental results. For the experimental results, the left path of tracer was not observed. The dye distribution may vary in the normal direction to the observation face of the box. This may need to be further examined with more experiments.

Figure 11 shows the concentration variation at different observation points. Although the concentration at observation points in the experiment did not show any response to the solute input except for point 3, the numerical results indicated changes in concentration. According to the experimental results, point 3 was in the main path of tracer transport. This point, however, did not show a large peak in concentration in the numerical results. The experimental result for point 1 revealed a constant concentration, while the numerical results indicated a fluctuating pattern of the concentration for the same point.

Figure 12 shows the numerical results for volumetric water content. The numerical results for water content almost agreed well with experimental results. But at point 3, numerical result could not reproduce experimental one.

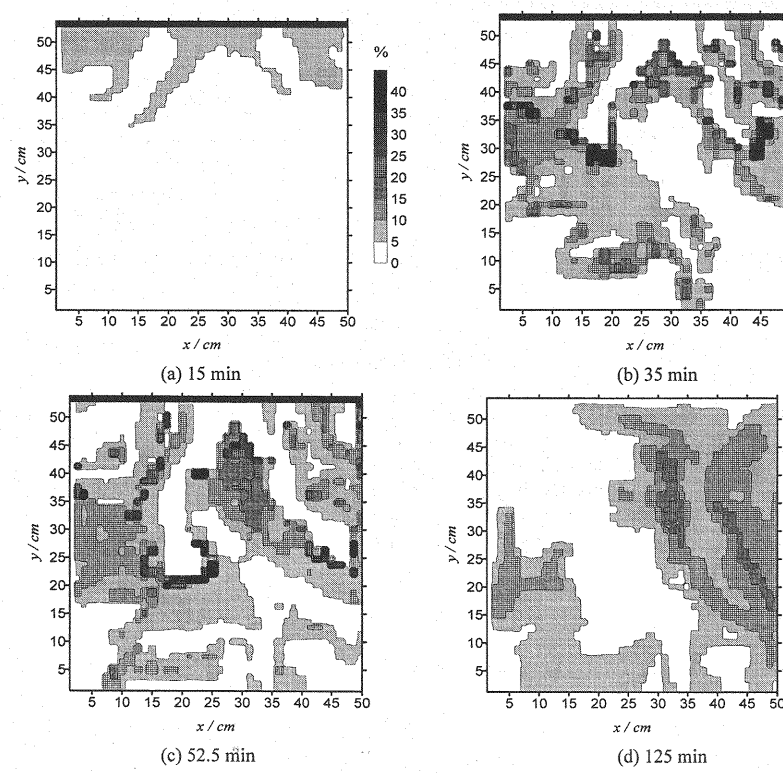

Figure 10 Calculated infiltration process

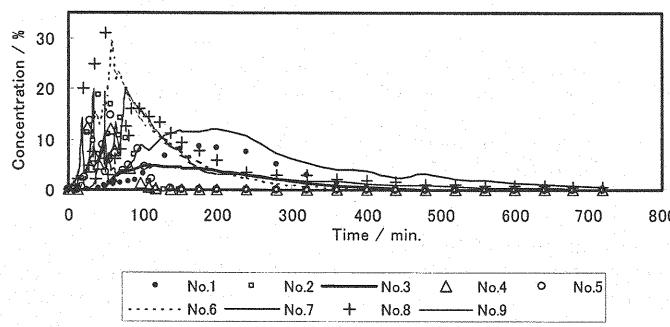

Figure 11 Numerical results of change in concentration

Figure 13 shows the temporal change in calculated pressure head at different observation points. The pressure head at point E suddenly rose, and was different from the experimental results. After an initial stage, the value became so constant that it resembled the experimental result, even if the values and the sign are different. In general calculation results showed that the temporal change in water content, pressure head, and concentration have similar tendencies as experimental results.

However, the difference between visualized main path of dye experiment and main tracer path of numerical results is observed. Preliminary air packed in the experimental box may affects water flow and tracer transport. Further examination will be needed in order to understand the phenomena more precisely.

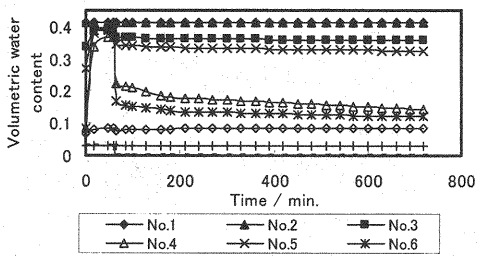

Figure 12 Numerical results of change in water content

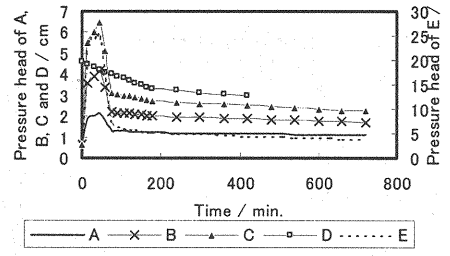

Figure 13 Numerical results of change in pressure head

CONCLUSIONS

In this study, laboratory experiments and numerical simulations were performed to obtain fundamental characteristics of water flow and solute transport in a heterogeneous hydraulic flow field. Water and solute moved preferentially due to the heterogeneous distribution of hydraulic conductivity and microscopic dispersivity. The qualitative tendency of numerical results for concentration, pressure head, and water content agreed with experimental results. However, the main tracer path in the numerical simulation was different from that in dye experiment. Because of this difference, further examination will be needed.

ACKOWLEDGEMENTS

The authors are grateful to Ronny Berndtsson of Lund University for reading the manuscript and for useful suggestions.

REFERENCES

1. Mantoglou, A.: A Theoretical Approach for Modeling Unsaturated Flow in Spatially Variable Soils: Effective Flow Models in Finite Domains and Nonstationarity, *Water Resources Research*, Vol.28, No.1, pp.251-267, 1992.
2. Jensen, K.H. and Mantoglou, A.: Application of Stochastic Unsaturated Flow Theory, Numerical Simulations, and Comparisons to Field Observations, *Water Resources Research*, Vol.28, No.1, pp.269-284, 1992.
3. Yeh, T.-C.J. and Harvey, D.J.: Effective Unsaturated Hydraulic Conductivity of Layered Sands, *Water Resources Research*, Vol.26, No.6, pp.1271-1279, 1990.
4. Sakamoto, Y.: Simulation of water path through unsaturated media by water path invention model involving effects of angle of contact and water content, *Annual Journal of Hydraulic Engineering*, vol.38, pp.179-184, 1994. (in Japanese with English abstract)
5. Sakamoto, Y.: Solute transport by water path flow through unsaturated media, *Annual Journal of Hydraulic Engineering*, vol.39, pp.337-342, 1995. (in Japanese with English abstract)
6. Nakagawa, K., K. Jinno, T. Hosokawa, K. Hatanaka, Y. Ijiri and S. Watari: Numerical study on non-reactive tracer transport in a heterogeneous field, with random microscopic dispersivity, *Groundwater Quality: Remediation and Protection* Herbert, M. and K. Kovar eds., IAHS Publication No.250, pp.567-574, 1998.
7. Nakagawa, K., K. Jinno, and T. Hosokawa: Microscopic and macroscopic dispersions in numerically generated heterogeneous porous media, *Journal of Hydroscience and Hydraulic Engineering*, Vol.18, No.1, pp.53-60, 2000.
8. Nakagawa, K. and K. Jinno: Evaluation of the transition characteristics of macroscopic dispersion and estimation of the non-uniform hydrogeological structure, *Calibration and Reliability in Groundwater Modelling: Coping with Uncertainty* Stauffer, F, W. Kinzelbach, K. Kover and E. Hoehn eds., IAHS Publication No.265, pp.110-116, 1999.
9. Wildenschild, D. and Jensen, K.H.: Laboratory investigations of effective flow behavior in unsaturated heterogeneous sands, *Water Resources Research*, Vol.35, No.1, pp.17-27, 1999.

10. Wildenschild, D. and Jensen, K.H.: Numerical modeling of observed effective flow behavior in unsaturated heterogeneous sands, *Water Resources Research*, Vol.35, No.1, pp.29-42, 1999.
11. Jinno, K. eds: *Numerical analysis of mass transport in groundwater*, Kyushu University Press, 2000. (in Japanese)
12. Clothier, B.E. and White, I.: Measurement of Sorptivity and Soil Water Diffusivity in the Field, *Soil Science Society of America Journal*, Vol.45, pp.241-245, 1981.
13. Huyakorn, P.S. and Pinder, G.F.: *Computational method in subsurface flow*, Academic Press, 1983.
14. van Genuchten, M.T.: A closed-form equation for predicting the hydraulic conductivity of unsaturated soils, *Soil Science Society of America Journal*, Vol.44, No.5, pp.892-898, 1980.

APPENDIX-NOTATION

The following symbols are used in this paper:

C	=	concentration of tracer;
c_W	=	specific moisture capacity;
D_M	=	fluid molecular diffusion coefficient;
D_{xx}, D_{yy}, D_{xy}, D_{yx}	=	dispersion coefficient;
h	=	piezometric head;
k	=	hydraulic conductivity;
k_s	=	saturated hydraulic conductivity;
S_S	=	specific storage coefficient;
t	=	time;
u, v	=	Darcy's velocity for x and y directions;
u', v'	=	pore water velocity for x and y directions;
V	=	pore water velocity for flow direction;
$\underline{Y}$	=	log-transformed hydraulic conductivity;
$\overline{Y}$	=	mean value of Y;
α, m and n	=	coefficients of van Genuchten formula;
α_L, α_T	=	microscopic dispersivity for longitudinal and transverse directions;
β	=	dummy number that takes 0 in unsaturated condition and 1 in saturated condition;
θ	=	volumetric water content;
θ_r	=	residual water content;
θ_s	=	saturated water content; *and*
σ_Y	=	standard deviation of Y.

(Received June 30, 2003 ; revised August 31, 2003)